JOURNAL OF COMPUTATIONAL PHYSICS 36, 135–153 (1980)

Finite Element Simulation of Flow in Deforming Regions

DANIEL R. LYNCH

Resource Policy Center, Thayer School of Engineering, Dartmouth College, Hanover, New Hampshire 03755

AND

WILLIAM G. GRAY

Water Resources Program, Department of Civil Engineering, Princeton University, Princeton, New Jersey 08540

Received September 6, 1978; revised July 11, 1979

A finite element technique for solving multidimensional flow problems with moving boundaries is developed by means of Galerkin's procedure. The method accounts automatically for continuous grid deformation during simulation, and utilizes finite difference techniques in the time domain. In the absence of grid deformation, the method reduces to the standard Galerkin finite element formulation. Utility of the approach is demonstrated by application to one- and two-dimensional flow problems.

INTRODUCTION

There are many engineering situations in which the flow of fluid in the vicinity of a moving boundary is of interest. Among the examples which are commonly encountered are vertical wave motion in open channels and containers, unconfined flow of groundwater, and propagation of tidal waves into dry coastal areas. These problems all share the feature that the spatial domain occupied by the fluid deforms during the course of motion, while the rate of boundary deformation at any time is determined by the state of the fluid at the boundary.

The finite element method has been applied successfully to many kinds of transient field problems, and several works on this subject are now available (Zienkiewicz, 1971; Oden *et al.*, 1974; Connor and Brebbia, 1976; Gray *et al.*, 1977; Pinder and Gray, 1977; Bathe *et al.*, 1977; Brebbia *et al.*, 1978). By far the bulk of this work pertains to problems with fixed domains. A common approach has been to use the Galerkin method to generate a set of ordinary differential equations in the time domain. Finite difference methods are typically used to integrate these equations in time, although other methods have been used to advantage (e.g., transform methods or finite element representations in time).

0021-9991/80/080135-19$02.00/0

In this paper, the Galerkin finite element method is applied in a way which allows the spatial domain to deform during simulation. The development parallels the conventional Galerkin approach, such that existing programs which treat only fixed boundary problems can readily be adapted to the moving boundary case. Although the concept of numerical simulation on a deforming grid is not entirely new, the present development is noteworthy insofar as it incorporates several important features at the outset: it is applicable to both parabolic and hyperbolic problems; the formulation is given for the general case of three space dimensions; and the method can readily be used with higher-order triangular and quadrilateral finite elements. Further, the flexibility of the finite difference formulation in time is preserved, allowing the use of a wide range of time-stepping schemes (including multilevel schemes). Since the method accounts automatically for arbitrary node motion, it applies to fixed boundary problems where it is necessary or expedient to allow internal mesh deformation, as well as to moving boundary problems.

Application of the method to the study of shallow water wave propagation is demonstrated. An existing two-dimensional model is modified to include the moving boundary effects arising from the flooding and dewatering of beaches and salt flats. The influence of the moving boundary on the circulation at and near the boundary is demonstrated.

Literature Review

Two basic approaches may be followed in simulating a moving boundary problem:

a. A straightforward application of existing methods for fixed spatial grids can be adopted. Special precautions must be taken both to recognize the location of the moving boundary at any point in time, and to approximate the physics at the boundary. Accuracy in the vicinity of a physically important moving boundary relies on high numerical resolution near the boundary. With nodes fixed in space, this high resolution must be maintained throughout that portion of the domain which "contains" the boundary motion for the entire simulation. In problems involving large boundary motions, considerable amounts of otherwise unnecessary numerical detail may be required. Nevertheless, provided a suitable numerical representation is used for the physics at the boundary, this approach is attractive insofar as it uses established numerical methods for fixed-grid problems.

b. Alternatively, moving boundary problems may be solved using a deforming numerical grid. Grid deformation must be such that node points at the perimeter of the numerical domain always coincide with the moving boundary. In the abstract, this approach has an intuitively greater appeal. The disadvantages are of course the practical and theoretical problems encountered in (i) ensuring that boundary nodes do in fact "track" the moving boundary, and (ii) accounting accurately for the effects of grid deformation.

Several authors have reported simulations of hyperbolic moving boundary problems. Reid and Bodine (1968) describe the finite difference solution of the two-dimensional shallow water equations, using a fixed mesh. Moving boundaries are approximated by turning finite-difference cells on and off at the boundary, and accounting for the conservation of mass in the process. Leendertse (1970) describes a similar fixed-grid finite difference approach. Boundary motion in both cases is characterized by impulsive jumps followed by periods of rest. An analogous approach using fixed-grid finite elements is reported by Holz and Withum (1977) for two-dimensional shallow water circulation. Difficulties related to the mass flux across the moving boundary are reported, and the authors suggest that inaccuracies near the boundary may be large. Xanthopoulos and Koutitas (1976) report a fixed-grid finite difference solution for two-dimensional overland flow, under kinematic conditions.

Boris *et al.* (1975) simulated free surface hydrodynamics in two dimensions using finite differences. A generalized triangular mesh was employed, and continuous node motion was allowed such that boundary nodes followed the motion of the free surface. Jamet and Bonnerot (1975) solved the compressible flow equations in one dimension using finite elements in both space and time. In effect this approach uses a continuously deforming spatial grid; the finite element treatment of the time domain accounts automatically for the effects of grid deformation.

Numerical solutions for parabolic moving boundary problems have been reported more extensively in the literature. A large portion of this work concerns Stefan-type problems, and several useful review articles are available (Crank, 1975; Fox, 1975; Meyer, 1978). Many investigators have used a finite difference approach, and these results have been summarized by Crank (1975). Generally speaking, both fixed and deforming finite difference grids have been used. Applications are largely confined to one-dimensional situations and frequently lack generality. Among the moving grid approaches, a common (although perhaps not insurmountable) problem would appear to be the distorted mesh which would result in higher-dimensional situations. The Isotherm Migration Method (Crank and Gupta, 1975) deserves special mention insofar as the roles of the dependent and one of the independent space variables are interchanged, allowing a fixed grid to be created in the temperature domain. Generalization of this procedure to other types of moving boundary problems, however, remains to be demonstrated.

Several finite element solutions of parabolic Stefan-type problems have also been reported. Comini *et al.* (1974) used a fixed mesh approach. Latent heat effects at the moving boundary were accounted for by a special device (the "apparent heat capacity"). Del Giudice *et al.* (1978) and Morgan *et al.* (1978) have reported improvements of this method. Goodrich (1978) has criticized this approach and has demonstrated its inferiority to a moving grid finite difference formulation for certain one-dimensional problems. Guymon and Luthin (1974) report a fixed-grid finite element approach in which freezing occurs simultaneously over a whole element when its hypothetical heat deficit equals the latent heat content. All of these fixed-grid finite element approaches are capable of handling higher-dimensional situations.

Bonnerot and Jamet (1974, 1977) solved the Stefan problem using finite elements in

both space and time. The approach is the same as that of Jamet and Bonnerot (1975). The spatial grid deforms continuously in time; the effects of this deformation are accounted for by the finite-element representation in time. One- and two-dimensional solutions are reported. Mori (1976a, b) also solved the Stefan problem using continuously deforming finite elements in space and finite difference techniques in the time domain. The effects of mesh deformation are accounted for by making the finite element basis functions implicit functions of time. Again, one- and two-dimensional solutions are reported.

Numerical solutions to parabolic moving boundary problems have also been reported in the area of groundwater flow. Neuman and Witherspoon (1971) report a two-dimensional finite-element model for free surface problems which uses continously deforming elements. Nakano (1978) developed a fixed-grid finite difference model for one-dimensional saturated/unsaturated flow.

Conceptually, the deforming grid approach to simulation of moving boundary problems is preferable to the fixed-grid approach, provided the details of grid deformation can be incorporated efficiently. Among the specific approaches outlined above, the space-time finite element formulation of Bonnerot and Jamet (1974, 1977) and Jamet and Bonnerot (1975) appears to be the most general, having been applied to both parabolic and hyperbolic problems. At least at present, most of the other formulations seem to be limited in various ways to particular types of applications.

An alternative to the space-time finite element approach is developed below. This approach also uses continuously deforming finite elements in the spatial domain, but retains the conventional finite difference formulation in time. The development, although broader in scope, initially parallels that of Mori (1976a). The resulting methodology, like the space-time finite element approach, is applicable to a very general class of moving boundary problems.

Galerkin Formulation on Deforming Finite Elements

Consider first the Galerkin finite element approach in cases where the boundaries are fixed. The problem to be solved, subject to the appropriate initial and boundary conditions, may be illustrated schematically as

$$Lu = f, \tag{1}$$

where

L	is a differential operator with derivatives in time and space,
$u(\mathbf{x}, t)$	is the unknown function,
$f(\mathbf{x}, t)$	is a known forcing function,
$\mathbf{x}$	is the set of independent space variables,
t	is time.

An approximate solution $\hat{u}(\mathbf{x}, t)$ is sought in terms of known basis functions $\phi_j(\mathbf{x})$:

$$u \simeq \hat{u} = \sum_{j=1}^{N} u_j(t)\, \phi_j(\mathbf{x}). \tag{2}$$

Because (2) is only an approximation, its substitution into (1) will produce a nonzero residual $r(\mathbf{x}, t)$:

$$L\hat{u} - f \equiv r(\mathbf{x}, t). \tag{3}$$

The Galerkin procedure requires the residual to be orthogonal to each of the basis functions ϕ_i:

$$\langle r(\mathbf{x}, t), \phi_i \rangle = 0, \qquad i = 1,..., N, \tag{4}$$

where $\langle , \rangle$ is the inner product notation. Equation (4) constitutes a set of ordinary differential equations in the time domain for the functions $u_j(t)$. Typically, these equations are integrated from the initial conditions by the use of finite difference approximations to (4) at discrete points in time t_k.

When moving boundaries are involved, this same general approach can be retained. Simulation begins with the specification of initial conditions on an initial finite element grid and marches forward in time, allowing nodes to move while maintaining their initial connectivity. At any time when the initial mesh becomes unacceptably distorted due to accumulated node movement, a rezoning of the domain is performed. This can be achieved by stopping the simulation and adding or deleting nodes as required, keeping the boundary location fixed. The simulation may then continue as an initial-value problem. Boundary motion and the associated grid deformation are thus achieved by the juxtaposition of two processes: incremental growth with fixed connectivity, and instantaneous rezoning with fixed boundaries. Both parts of this problem must be accomplished accurately and efficiently to obtain a good solution. Incremental growth occurs during each time step and requires an effective equation solution technique; this process is the major concern of this paper. The rezoning process implies automatic recognition of mesh distortion as well as the rezoning itself, both of which are nontrivial programming problems. However, these problems appear to be solvable by an efficient bookkeeping system similar to that used in automatic mesh generation and are not dealt with herein.

Within this general framework, then, the moving boundary problem can be approached by extending the basic Galerkin formulation to account for mesh deformation. Three modifications are required in the general formulation (4) to account for node motion. First, since the value of a basis function ϕ_j at any point depends upon the locations of the nodes, ϕ_j becomes an implicit function of time:

$$\phi_j = \phi_j(\mathbf{x}, \mathbf{X}_l(t)) = \phi_j(\mathbf{x}, t), \tag{5}$$

where the $\mathbf{X}_l(t)$ are the node coordinates. Also, the domain of integration implied by the inner product notation changes with time. The set of equations (4) thus become

nonstationary as well as nonlinear. (For example, the mass matrix $\langle \phi_j, \phi_i \rangle$ which normally multiplies the vector of time derivatives du_j/dt is no longer constant in time.)

Second, equations for node motion must be added to set (4). Each nodal position $\mathbf{X}_l(t)$ must be integrated from initial conditions by use of the identity

$$\frac{d}{dt}\mathbf{X}_l(t) = \mathbf{V}_l(t), \tag{6}$$

where $\mathbf{V}_l$ is the velocity of node l. If node l is on the moving boundary, $\mathbf{V}_l$ is obtained from the boundary condition appropriate to the problem being solved, and will in general be related to the state of the fluid at the boundary. For interior nodes, either $\mathbf{V}_l = 0$ or $\mathbf{V}_l = \mathbf{v}_l$, where $\mathbf{v}_l$ is the fluid velocity at node l, would seem to be a natural choice, but in general the motion of interior nodes may be arbitrarily specified to suit the application.

The third departure from the conventional Galerkin approximation concerns the form of the time derivatives. When node motion is allowed, the approximate solution $\hat{u}(\mathbf{x}, t)$ takes the form

$$\hat{u}(\mathbf{x}, t) = \sum_{j=1}^{N} u_j(t)\, \phi_j(\mathbf{x}, t). \tag{7}$$

Note that this formulation identifies $u_j(t)$ as the value of $\hat{u}$ at node j, i.e., at the moving point $\mathbf{X}_j(t)$, throughout the simulation. While spatial derivatives of $\hat{u}$ will take their usual form, additional terms are generated when (7) is differentiated with respect to time:

$$\frac{\partial \hat{u}}{\partial t} = \sum_{j=1}^{N} \frac{du_j}{dt}\, \phi_j + \sum_{j=1}^{N} u_j \frac{\partial \phi_j}{\partial t}. \tag{8}$$

The first set of terms in (8) is the usual approximation for the time derivative in finite element models. The terms involving $\partial \phi_j/\partial t$ are nonzero only in elements which are deforming, and account for the rate of deformation of the spatial grid.[1] When second derivatives with respect to time appear in L, two sets of extra terms arise:

$$\frac{\partial^2 \hat{u}}{\partial t^2} = \sum_{j=1}^{N} \frac{d^2 u_j}{dt^2}\, \phi_j + 2 \sum_{j=1}^{N} \frac{du_j}{dt} \frac{\partial \phi_j}{\partial t} + \sum_{j=1}^{N} u_j \frac{\partial^2 \phi_j}{\partial t^2}. \tag{9}$$

In elements which are not deforming, Eq. (9) also reduces to the usual finite element approximation.

Evaluation of the weighted residuals (4) involves integration over the entire spatial domain (which is changing with time), and thus the terms $\partial \phi_j/\partial t$ and $\partial^2 \phi_j/\partial t^2$ must be defined throughout the domain. It is clear that these terms depend entirely upon the node locations $\mathbf{X}_l(t)$ and their derivatives. Expressions can thus in principle be

[1] Mori (1976a, b) has noted the presence of these terms in the expression for $\partial \hat{u}/\partial t$.

obtained by writing the basis functions in terms of $\mathbf{X}_i(t)$ and differentiating.[2] However, this is a tedious procedure for all but the simplest elements, and a simple general relation can be obtained for any isoparametric element as follows.

Consider, for example, a special case of a two-dimensional isoparametric element (Fig. 1) which will be allowed to deform. To perform the necessary integrations over this element it is usually transformed from the global (x, y) domain to a (ξ, η) domain in which it is a square, and in which the basis functions depend on ξ and η only (Ergatoudis *et al.*, 1968). Because the (ξ, η) space does not deform with time, the value of a basis function $\phi_i(\xi, \eta)$ at any point (ξ_0, η_0) will be constant in time. However, the point in the x, y domain which corresponds to (ξ_0, η_0) will depend upon time and the isoparametric transformation is of the form

$$\mathbf{x}(t) = \sum_{i=1}^{M} \mathbf{X}_i(t)\, \phi_i(\xi, \eta). \tag{10}$$

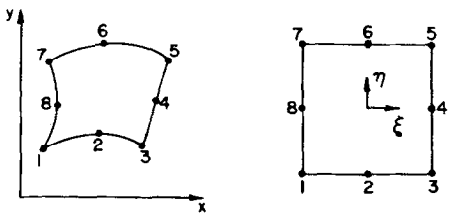

FIG. 1. Isoparametric quadrilateral in global and local coordinates.

Differentiation of this expression with respect to time at a particular ξ, η location yields

$$\frac{d\mathbf{x}}{dt} = \sum_{i=1}^{M} \frac{d\mathbf{X}_i}{dt}\, \phi_i(\xi, \eta) = \sum_{i=1}^{M} \mathbf{V}_i(t)\, \phi_i(\xi, \eta) \equiv \mathbf{V}^e, \tag{11}$$

where $\mathbf{V}^e$ will be referred to as the elemental velocity. An observer moving at the elemental velocity will detect no change in ϕ_i so

$$\frac{d\phi_i}{dt} = \frac{\partial \phi_i}{\partial t} + \mathbf{V}^e \cdot \nabla \phi_i = 0. \tag{12}$$

Equation (12) provides a simple determination of $\partial \phi_i / \partial t$ at any point in $(\mathbf{x}, t)$ and for any isoparametric element, in terms of the nodal velocities and the spatial gradients of ϕ_i. Since these gradients are used throughout any finite element program, no new complications are introduced. (The above analysis is readily applied to isoparametric triangular elements by substituting the triangular area coordinates for ξ and η.)

[2] Mori (1976a) has used this approach in evaluating $\partial \phi_i / \partial t$ for one-dimensional linear elements.

Use can be made of (12) to simplify the expression obtained for the time derivative as given in Eq. (8). Substitution of (12) into (8) yields

$$\frac{\partial \hat{u}}{\partial t} = \sum_{j=1}^{N} \frac{du_j}{dt} \phi_j - \mathbf{V}^e \cdot \sum_{j=1}^{N} u_j \nabla \phi_j . \tag{13}$$

However,

$$\sum_{j=1}^{N} u_j \nabla \phi_j = \nabla \sum_{j=1}^{N} u_j \phi_j = \nabla \hat{u}. \tag{14}$$

Therefore (13) becomes

$$\frac{\partial \hat{u}}{\partial t} = \sum_{j=1}^{N} \frac{du_j}{dt} \phi_j - \mathbf{V}^e \cdot \nabla \hat{u}. \tag{15}$$

The additional term in (15) which accounts for nodal motion can be interpreted as a correction for the Lagrangian nature of approximation (7) in elments which are deforming.

The expression for $\partial^2 \phi_i / \partial t^2$ obtained by differentiation of (12) is

$$\frac{\partial^2 \phi_i}{\partial t^2} = -\left[\sum_{j=1}^{N} \frac{d\mathbf{V}_j}{dt} \phi_j\right] \cdot \nabla \phi_i + 2\mathbf{V}^e \cdot (\nabla \mathbf{V}^e) \cdot \nabla \phi_i + \mathbf{V}^e \cdot (\nabla \nabla \phi_i) \cdot \mathbf{V}^e. \tag{16}$$

Although (16) appears to be more complicated than (12) it allows for simple computation of $\partial^2 \phi_i / \partial t^2$, given the nodal velocities and accelerations.

The general results (16) and (12), coupled with (8) and (9), form the foundation of our approach to finite element simulation on a deforming mesh.

Application to Shallow Water Problems

As an illustration, the approach outlined above has been applied to the simulation of circulation in shallow, vertically homogeneous coastal regions. The horizontal fluid motion in such areas can be described by the shallow water equations, which are obtained by vertical integration of the equations of continuity and motion (Pritchard, 1971). Further manipulation of these equations yields the shallow water wave equation (Lynch and Gray, 1979)

$$\frac{\partial^2 H}{\partial t^2} + \tau \frac{\partial H}{\partial t} = \nabla \cdot (gH \nabla \zeta) + H\mathbf{v} \cdot \nabla \tau + \nabla \cdot [\nabla \cdot (H\mathbf{v}\mathbf{v}) + \mathbf{f} \times H\mathbf{v} - \mathbf{W}], \tag{17a}$$

which may be solved in conjunction with the primitive horizontal momentum equation

$$\frac{\partial \mathbf{v}}{\partial t} = -\mathbf{v} \cdot \nabla \mathbf{v} - \mathbf{f} \times \mathbf{v} - g \nabla \zeta - \tau \mathbf{v} + \frac{\mathbf{W}}{H}, \tag{17b}$$

where

$H(\mathbf{x}, t)$	is the total fluid depth,
$\zeta(\mathbf{x}, t)$	is the elevation of the free surface above a reference datum,
$h(\mathbf{x})$	is the bathymetry: $h = H - \zeta$,
$\mathbf{v}(\mathbf{x}, t)$	is the vertically averaged horizontal fluid velocity,
$\mathbf{f}$	is the Coriolis parameter,
g	is gravity,
$\mathbf{W}(\mathbf{x}, t)$	is the wind stress,
$\tau\mathbf{v}(\mathbf{x}, t) = (g \mid \mathbf{v} \mid \mathbf{v})/(C^2 H)$	is the bottom stress,
$C(\mathbf{x}, t)$	is the Chezy coefficient,
$\mathbf{x}$	is the set of two horizontal spatial coordinates,
t	is time.

Equations (17) are hyperbolic, and two types of boundary conditions have typically been considered: the specification of fluid depth on fixed boundaries, or alternatively the specification of fluid velocity normal to fixed boundaries. There is, however, a third type of condition, where the depth is required to be zero on shoreline boundaries which follow the motion of the fluid:

$$H = 0 \qquad \text{on} \qquad \mathbf{X} = \mathbf{X}_0 + \int_0^t \mathbf{V}\, dt; \qquad \mathbf{V} = \mathbf{v}, \tag{18}$$

where $\mathbf{X}(t)$ is the location of the boundary at time t, $\mathbf{X}_0$ is the initial boundary location, and $\mathbf{V}$ is the velocity of the boundary. While the first two types of BC's are adequate for solution of a variety of practical problems, the details of fluid motion in the vicinity of a moving boundary are often the most important aspects of a solution, and may in fact be the motivation for the modeling effort. Examples include coastal sedimentation and erosion.

A numerical solution to (17) may be sought in the finite-element form

$$H(\mathbf{x}, t) \simeq \sum_{j=1}^{N} H_j(t)\, \phi_j(\mathbf{x}, t), \tag{19a}$$

$$\mathbf{v}(\mathbf{x}, t) \simeq \sum_{j=1}^{N} \mathbf{v}_j(t)\, \phi_j(\mathbf{x}, t), \tag{19b}$$

$$\tau(\mathbf{x}, t) \simeq \sum_{j=1}^{N} \tau_j(t)\, \phi_j(\mathbf{x}, t). \tag{19c}$$

Substitution of approximations (19) into (17) and setting the weighted residuals to zero yield the set of ordinary differential equations

$$\sum_{j=1}^{N} \left[\frac{d^2 H_j}{dt^2} \langle \phi_j , \phi_i \rangle + 2 \frac{dH_j}{dt} \left\langle \frac{\partial \phi_j}{\partial t} , \phi_i \right\rangle + H_j \left\langle \frac{\partial^2 \phi_j}{\partial t^2} , \phi_i \right\rangle \right.$$
$$\left. + \frac{dH_j}{dt} \langle \tau \phi_j , \phi_i \rangle + H_j \left\langle \tau \frac{\partial \phi_j}{\partial t} , \phi_i \right\rangle \right] = \langle R_W , \phi_i \rangle, \tag{20a}$$

$$\sum_{j=1}^{N} \left[\frac{d\mathbf{v}_j}{dt} \langle \phi_j , \phi_i \rangle + \mathbf{v}_j \left\langle \frac{\partial \phi_j}{\partial t} , \phi_i \right\rangle \right] = \langle \mathbf{R}_M , \phi_i \rangle, \qquad i = 1, \ldots, N, \tag{20b}$$

where $R_W(\mathbf{x}, t)$ and $\mathbf{R}_M(\mathbf{x}, t)$ are the right-hand sides of Eqs. (17a) and (17b), respectively, with approximations (19) substituted for the exact values.

Application of the finite-difference approach in time requires that Eqs. (20) be satisfied approximately at discrete points in time. Use of a three-level scheme is required by the second derivatives in (20a) and allows an explicit formulation which is centered in time. Simple second-order correct approximations for the time derivatives may be used:

$$\left. \frac{d^2 H_j}{dt^2} \right|_t \simeq \left[\frac{H_{t+\Delta t} - 2H_t + H_{t-\Delta t}}{\Delta t^2} \right]_j , \tag{21a}$$

$$\left. \frac{dH_j}{dt} \right|_t \simeq \left[\frac{H_{t+\Delta t} - H_{t-\Delta t}}{2\Delta t} \right]_j , \tag{21b}$$

$$\left. \frac{d\mathbf{v}_j}{dt} \right|_t \simeq \left[\frac{\mathbf{v}_{t+\Delta t} - \mathbf{v}_{t-\Delta t}}{2\Delta t} \right]_j . \tag{21c}$$

Substitution of (21) into (20) and evaluation of the inner products and the terms R_W and $\mathbf{R}_M$ at time t, yield a time-stepping scheme for the values of H_j and $\mathbf{v}_j$ at time $t + \Delta t$.

In the absence of nodal motion, this model reduces to the explicit wave equation model, which has been shown to produce excellent results for a range of problems involving fixed boundaries (Lynch and Gray, 1979). In linearized, one-dimensional form, the model is governed by the stability constraint[3]

$$gH \left(\frac{\Delta t}{\Delta x} \right)^2 \leqslant \frac{1}{3} . \tag{22}$$

When moving boundaries are introduced, the motion of each node must be defined to complete the model. Generally speaking, it is desirable to minimize unnecessary node motion, since it is computationally efficient to keep the grid as stationary as

[3] Evaluation of the friction term in $\mathbf{R}_M$ at time t leads to a computational instability. In the results reported below, this friction term is evaluated at time $t - \Delta t$. This procedure introduces an additional stability constraint: $\tau \Delta t \leqslant 1$. Lynch and Gray (1979) discuss this point and also give an alternative method for avoiding this instability which eliminates the additional constraint.

possible. In particular for shallow water problems it is reasonable to keep interior nodes fixed. This has the advantage of allowing the bathymetry function, which is often a major determinant of initial node placement, to remain fixed over most of the domain. Furthermore, the numerical method reduces to its proven stationary equivalent in most of the elements. Once interior node positions are fixed, tangential motion of boundary nodes could cause unnecessary computational difficulties due to the shearing of boundary elements. Thus it is generally desirable to eliminate this tangential motion, where possible.

Consideration of Eq. (18) leads to the realization that if $\mathbf{V} = \mathbf{v}$ along the boundary, element shearing can become quite significant. However, to ensure conservation of mass it is only necessary that the normal components of the boundary and fluid velocities be equal. Thus (18) can be restated in a less restrictive form:

$$H = 0 \qquad \text{on} \qquad \mathbf{X} = \mathbf{X}_0 + \int_0^t \mathbf{V}\, dt; \qquad (\mathbf{V} - \mathbf{v}) \cdot \mathbf{n} = 0, \tag{23}$$

where $\mathbf{V}$ and $\mathbf{v}$ are the boundary and fluid velocities, respectively, and $\mathbf{n}$ is a unit vector normal to the boundary. The tangential velocity of the boundary nodes may be set to any convenient values.

One final detail must be taken care of: in general, the discretized finite element domain will have a discontinuous normal direction at the junction of two boundary elements. It is therefore not possible to satisfy the normal velocity relation in (23) exactly at every point on the boundary. In a manner similar to that used for fixed boundaries, (Pinder and Gray, 1977) relation (23) can be required to hold in an average sense for the computed velocities:

$$\int_S (\mathbf{V} - \mathbf{v}) \cdot \mathbf{n}\, dS = 0, \tag{24}$$

where S is the moving boundary. Expression of these velocities in terms of the finite element basis functions yields

$$\mathbf{V} \simeq \sum_i \mathbf{V}_i \phi_i\,, \tag{25a}$$

$$\mathbf{v} \simeq \sum_i \mathbf{v}_i \phi_i\,. \tag{25b}$$

Substitution of these expressions into (24) gives the relation

$$\sum_i \int_S (\mathbf{V}_i - \mathbf{v}_i) \cdot \mathbf{n} \phi_i\, dS = 0. \tag{26}$$

The most local way to satisfy (26) is to require each term in the summation to equal zero, or

$$(\mathbf{V}_i - \mathbf{v}_i) \cdot \int_S \mathbf{n} \phi_i\, dS = 0, \tag{27}$$

which serves as a definition of the nodal normal direction $\mathbf{n}_i$:

$$\mathbf{n}_i \equiv \frac{\int_S \mathbf{n}\phi_i \, dS}{\left| \int_S \mathbf{n}\phi_i \, dS \right|} \tag{28}$$

when node i is at the junction of two moving boundary segments. This definition is identical to that proposed by Gray (1977) and Pinder and Gray (1977) for fixed boundaries, and which has been used successfully in the wave equation models by Lynch and Gray (1979). Evaluation of (28) is facilitated by use of the divergence theorem:

$$\int_S \mathbf{n}\phi_i \, dS = \iint_A \nabla\phi_i \, dA, \tag{29}$$

where A is the entire spatial domain (Gray, 1977). Thus, evaluation of the nodal normal direction at any point in time does not present any new difficulties. It must be remembered, however, that for moving boundary problems the nodal normals change as the simulation proceeds, due to mesh distortion. It is useful to point out that for the special case of linear triangular elements, the nodal normal is perpendicular to the line AC in Fig. 2.

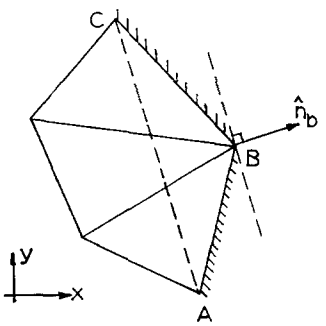

FIG. 2. Portion of a triangular grid with average nodal normal indicated for node B.

The final numerical form of the moving boundary condition (18) is thus

$$H_i = 0 \quad \text{on} \quad \mathbf{X}_i = \mathbf{X}_{i0} + \int_0^t \mathbf{V}_i \, dt; \quad (\mathbf{V}_i - \mathbf{v}_i) \cdot \mathbf{n}_i = 0, \tag{30a}$$

$$\mathbf{V}_i \cdot \boldsymbol{\lambda}_i = 0, \tag{30b}$$

where the subscript i ranges over all moving boundary nodes, and $\boldsymbol{\lambda}_i$ is the tangential direction at node i. (Constraint (30b) is arbitrarily employed to reduce element shearing.)

All of the relations required by the model are now available, and a typical time step proceeds as follows. At time t, the nodal normal directions are computed based on the existing grid, using Eq. (28), and the boundary node velocities are determined in

accordance with (30). The node locations $\mathbf{X}_{i,t+\Delta t}$ can be extrapolated by a finite-difference approximation to (30a):

$$\mathbf{X}_{i,t+\Delta t} \simeq \mathbf{X}_{i,t-\Delta t} + 2\Delta t\, \mathbf{V}_{i,t} \tag{31}$$

and the term $d\mathbf{V}_i/dt$, required for computation of $\partial^2\phi_j/\partial t^2$, can likewise be approximated:

$$\left.\frac{d\mathbf{V}_i}{dt}\right|_t = \left.\frac{d^2\mathbf{X}_i}{dt^2}\right|_t \simeq \frac{\mathbf{X}_{i,t+\Delta t} - 2\mathbf{X}_{i,t} + \mathbf{X}_{i,t-\Delta t}}{\Delta t^2}. \tag{32}$$

With this information, all of the required terms in Eqs. (20) can be evaluated. Thus the values of the dependent variables H_i and $\mathbf{v}_i$ may be obtained at time $t + \Delta t$. The new nodal normals can then be computed based on the deformed grid, and the entire procedure repeated.

Numerical Results

Two moving boundary problems have been solved using the method described above. The matrices on the left side of Eqs. (20) were reformulated during every time step. All inner products were evaluated exactly, using formulas given by Zienkiewicz (1971) and Pinder and Gray (1977). The complete nonlinear equations were used in both problems, although the Coriolis effect was neglected in the first problem. The discretization in space and time for both problems is based on that used by Lynch and Gray (1979), which has produced a high degree of accuracy for similar fixed boundary problems with the same numerical model.

One numerical difficulty not mentioned in the model development is the characterization of bottom friction at the moving boundary. The most common formulation in shallow water problems, and the one used in this study, is the Manning–Chezy formula for the friction slope $\mathbf{S}_f$:

$$g\mathbf{S}_f = \frac{g\,|\,\mathbf{v}\,|\,\mathbf{v}}{C^2H} \equiv \tau(\mathbf{x}, t)\mathbf{v}. \tag{33}$$

The term τ, although finite throughout the interior of the domain, approaches infinity at the moving boundary, where $H = 0$. This suggests that the Manning–Chezy formulation breaks down near the moving boundary, and it is believed that basic hydraulic research is required in this area. For the present, however, there appears to be no alternative to this formulation. In the numerical scheme used herein, the function $\tau(\mathbf{x}, t)$ is expanded in terms of its nodal values τ_j and the finite-element basis functions (Eq. (19c)). The value assigned to τ_j at a boundary node must be representative of the frictional effect throughout the boundary element. A convention is required whereby the determination of τ_j at boundary nodes is based on some small,

positive depth. Preliminary numerical experiments have shown that good results are obtained when this friction depth is approximated with an average depth in the boundary elements, and this approach has been adopted in the example problems.

The first example involves a canal with linear bathymetry (Fig. 3a) subject to periodic forcing at the seaward end:

$$\zeta(x = 0, t > 0) = \sin(\omega t).$$

This problem was solved using two-dimensional linear triangles as in Fig. 3b, with $\Delta x = \Delta y = 5 \times 10^4$ ft, $H_0 = 30.$ ft, $\Delta t = 0.062$ hr, and $2\pi/\omega = 12.4$ hr. The Chezy coefficient in the friction term τ, Eq. (33), was computed according to Manning's formula

$$C_i = 1.49 H_i^{1/6}/n. \tag{34}$$

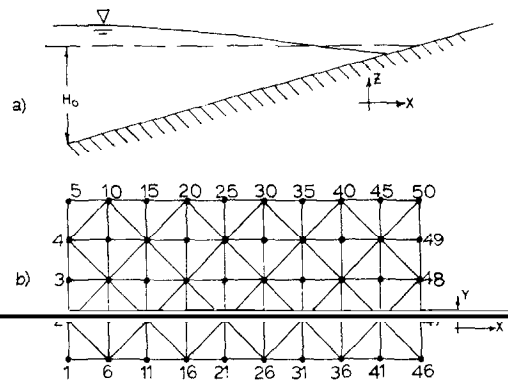

FIG. 3. (a) Linear bathymetry of a canal. (b) Triangular finite element grid for canal.

The value of n used was 0.035. The Coriolis effect was not included, and the friction depth at the moving boundary was chosen to be 1.0 ft. The moving boundary condition was applied at the landward boundary, and the solution compared to that obtained by applying a no-flux condition at $x = 8\Delta x$. The effect of this approximate no-flux boundary condition is expected to be greatest at the boundary, and it is reasonable to expect the two solutions to be equivalent at points well removed from the boundary. The dynamic steady-state responses at and near the boundary, obtained during the fifth tidal cycle after cold start, are shown in Figs. 4a and b.

Figure 4a shows the boundary surface elevation responses for the no-flux condition (node 45) and for the moving boundary (nodes 45 and 50). The two responses at node 45 are similar, being almost equal in phase, but differing by about a factor of 2 in amplitude. If only the no-flux boundary solution were available, a possible way to estimate the actual position of the shoreline would be to extrapolate the surface elevation at node 45 horizontally inland. Figure 4a reveals that this procedure yields

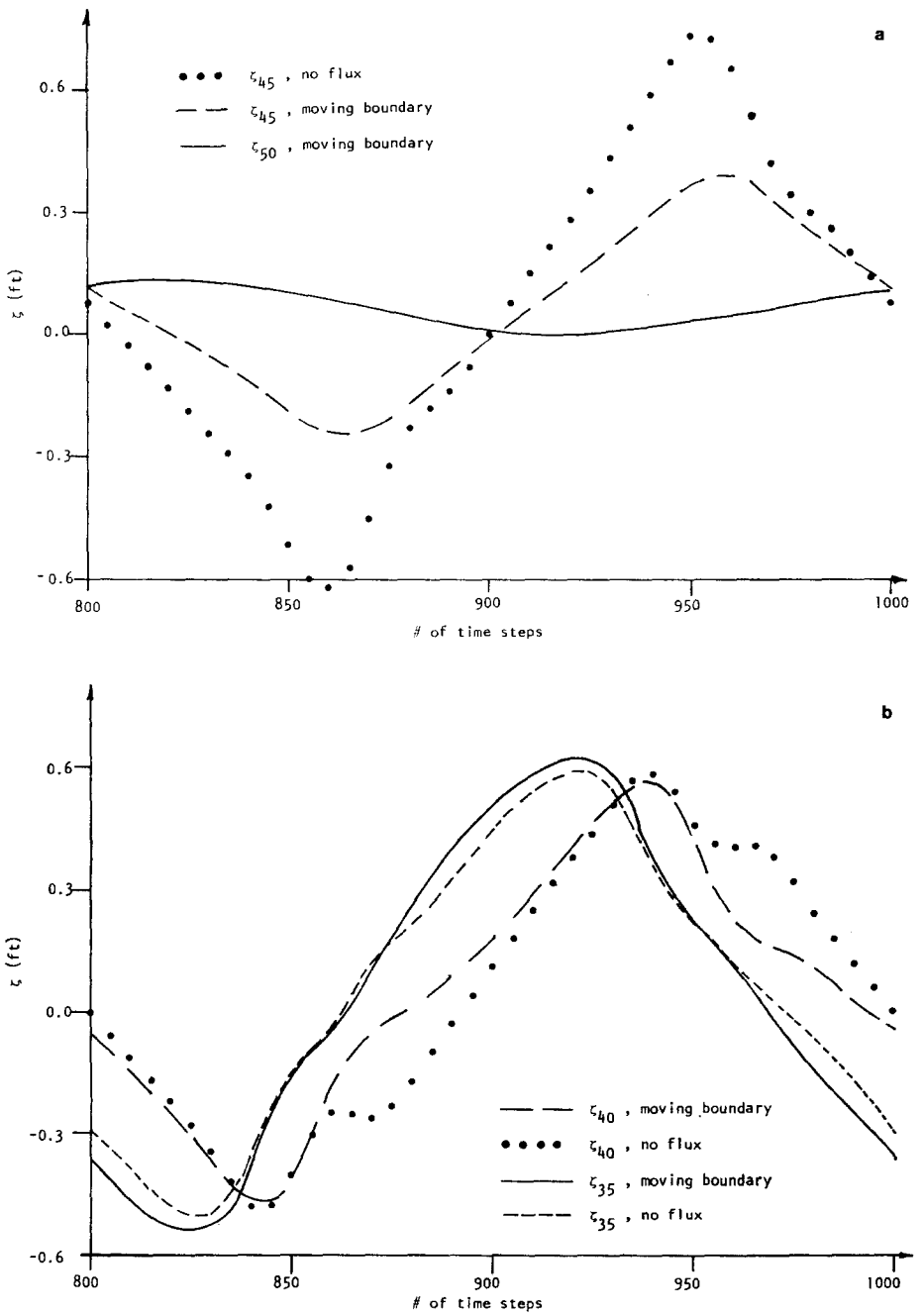

FIG. 4. (a) Surface elevation at boundary of the canal. (b) Surface elevation near boundary of the canal.

severe errors in both the amplitude and phase of the boundary motion. The heavy frictional losses and delay experienced by the boundary fluid while moving inland are not properly accounted for in the no-flux solution.

Figure 4b shows the surface elevation responses further in from the boundary at nodes 40 and 35. The agreement in phase continues to be good, and the discrepancy in amplitude decreases with distance from the boundary. The responses at node 20, well removed from the boundary, are practically indistinguishable, as expected.

The second moving boundary problem which has been considered involves a rectangular bay, illustrated in Fig. 5a. The bathymetry depends on y alone, and varies linearly as shown in Fig. 5b. This problem was solved using linear triangular elements, and the grid shown in Fig. 3b was employed. At $t = 0$, the harbor was taken to be at rest. At the harbor entrance (nodes 1, 6, 11) a storm surge was imposed:

$$\zeta(y = 0, t > 0) = 1.0 - \exp(-rt), \qquad 0 \leqslant x \leqslant 2\Delta x.$$

The boundary at $y = 4\Delta y$ (nodes 5, 10, 15,..., 50) was treated as a moving boundary, while the rest of the boundary was subject to the no-flux condition. Parameters used

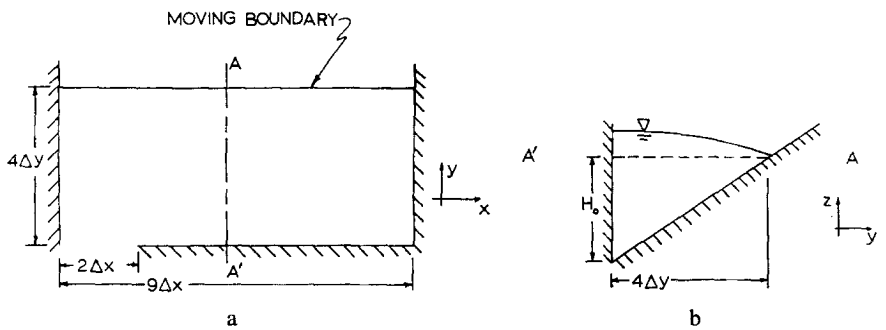

FIG. 5. (a) Harbor with moving boundary. (b) Harbor bathymetry, section A–A′.

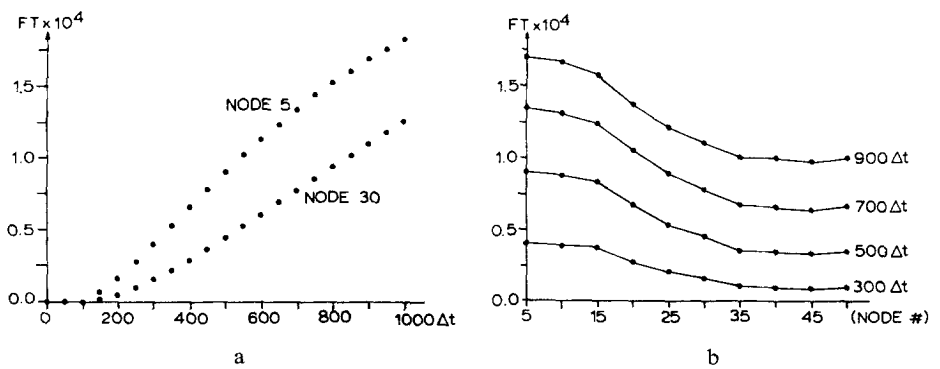

FIG. 6. (a) Node positions vs. time on moving boundary. (b) Moving boundary displacement at selected times.

were $\Delta x = \Delta y = 5. \times 10^4$ ft, $\Delta t = 0.062$ hr, $r = 0.333$ hr^{-1}, $n = 0.035$, and $H_0 = 8.0$ ft. At the moving boundary, the friction was computed based on a depth of 1.0 ft. As in the previous example all the nonlinear terms were retained. Coriolis acceleration was also included in this problem, equivalent to a latitude of 41° north.

Results obtained are shown in Figs. 6 and 7. In Fig. 6a the position of the moving boundary is plotted versus time for nodes 5 and 30. In Fig. 6b, the shape of the moving boundary is plotted at different points in time. Both of these figures show the expected behavior: the response is fastest at boundary points closest to the harbor entrance, and resembles a delayed exponential rise.

In Fig. 7, the velocity field obtained is plotted at time = 700 Δt and 900 Δt. The computed velocities behave as expected and in general are quite reasonable.

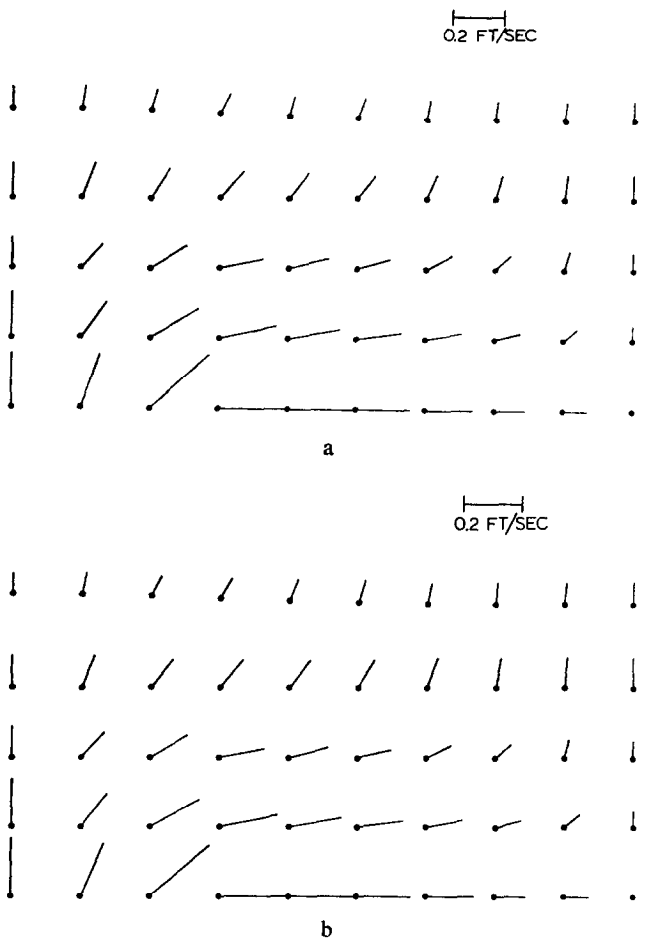

FIG. 7. (a) Velocity field at time of 43.4 hr (700 Δt). (b) Velocity field at time of 55.8 hr (900 Δt).

CONCLUSION

The Galerkin method can be readily applied to finite element simulation problems in which the spatial grid deforms in time. The resulting set of ordinary differential equations reduces to the standard Galerkin finite-element formulation in elements which experience no deformation. Node motion introduces extra terms which can be interpreted as corrections to the time derivatives due to the Lagrangian nature of the finite element approximations. These correction terms are readily evaluated using standard finite element procedures, and thus are easily incorporated into existing programs which treat only fixed-grid problems. Simulation of moving boundary problems can be accomplished by coupling the node motion to the state of the fluid by means of the boundary condition.

Application of this method has been demonstrated for coastal circulation problems where the shallow water equations govern. The solutions obtained are reasonable and well-behaved, and the introduction of the moving boundary appears to add no new instabilities to the basic finite element formulation of this problem. The moving boundary condition has a marked effect on the solution near the boundary, and the results have indicated that further basic research is needed in the characterization of boundary friction.

In this application, the flexibility associated with the finite difference formulation in time is quite important. All of the finite difference expressions used, including those which approximate the moving boundary condition, are centered in time and thus second-order correct; nevertheless, the specific formulation chosen allows time stepping to proceed explicitly, i.e., without iteration.

REFERENCES

K. J. BATHE, J. T. ODEN, AND W. WUNDERLICH, Eds. (1977), "Formulations and Computational Algorithms in Finite Element Analysis: U.S.–Germany Symposium," Massachusetts Institute of Technology, Cambridge, Mass.

R. BONNEROT AND P. JAMET (1974), *Int. J. Numer. Meth. Eng.* **8**, 811–820.

R. BONNEROT AND P. JAMET (1977), *J. Comput. Phys.* **25**, 163.

J. P. BORIS, K. L. HAIN, AND M. J. FRITTS (1975), *in* "Proceedings, First International Conference on Numerical Ship Hydrodynamics," David W. Taylor Naval Ship R & D Center, Bethesda, Md.

C. A. BREBBIA, W. G. GRAY, AND G. F. PINDER, Eds. (1978), "Finite Elements in Water Resources—2," Pentech Press, London, 1978.

G. COMINI, S. DEL GIUDICE, R. W. LEWIS, AND O. C. ZIENKIEWICZ (1974), *Int. J. Numer. Meth. Eng.* **8**, 613.

J. J. CONNOR AND C. A. BREBBIA (1976), "Finite Element Techniques for Fluid Flow," Newnes–Butterworth, London.

J. CRANK (1975), *in* "Moving Boundary Problems in Heat Flow and Diffusion" (J. R. Ockendon and W. R. Hodgkins, Eds.), Oxford Univ. Press (Clarendon), Oxford.

J. CRANK AND R. S. GUPTA (1975), *Int. J. Heat Mass Transfer* **18**, 1101.

S. DEL GIUDICE, G. COMINI, AND R. W. LEWIS (1978), *Int. J. Numer. Anal. Meth. Geomech.* **2**, 223.

I. ERGATOUDIS, B. M. IRONS, AND O. C. ZIENKIEWICZ (1968), *Int. J. Solids Struct.* **4**, 31–42.

L. FOX (1975), *in* "Moing Boundary Problems in Heat Flow and Diffusion (J. R. Ockendon and W. R. Hodgkins, Eds.), Oxford Univ. Press (Clarendon), Oxford.

L. E. GOODRICH (1978), *Int. J. Heat Mass Transfer* **21**, 615–621.
W. G. GRAY (1977), *in* "Finite Elements in Water Resources, I" (W. G. Gray, G. F. Pinder, and C. A. Brebbia, Eds.), Pentech Press, London.
W. G. GRAY, G. F. PINDER, AND C. A. BREBBIA, Eds. (1977), "Finite Elements in Water Resources, I," Pentech Press, London.
G. L. GUYMON AND J. L. LUTHIN (1974), *Water Resour. Res.* **10**, 995.
K. P. HOLZ AND D. WITHUM (1977), *in* "Formulations and Computational Algorithms in Finite Element Analysis: U.S.–Germany Symposium" (K. J. Bathe *et al.*, Eds.), Massachusetts Institute of Technology, Cambridge, Mass.
P. JAMET AND R. BONNEROT (1975), *J. Comput Phys.* **18**, 21–45.
J. J. LEENDERTSE (1970), "A Water Quality Simulation Model for Well-Mixed Estuaries and Coastal Seas: Volume 1, Principles of Computation," Rand Corp. Memorandum #RM-6230-RC.
D. R. LYNCH AND W. G. GRAY (1979), *Computers and Fluids* **1**, 207–228.
G. H. MEYER (1978), *in* "Moving Boundary Problems" (D. G. Wilson, A. D. Solomon, and P. T. Boggs, Eds.), Academic Press, New York.
K. MORGAN, R. W. LEWIS, AND O. C. ZIENKIEWICZ (1978), *Int. J. Numer. Meth. Eng.* **12**, 1191.
M. MORI (1976a), "A Finite Element Method for Solving Moving Boundary Problems," pp. 167–171, International Federation for Information Processing Conference on Modeling of Environmental Systems, Tokyo.
M. MORI (1976b), *Publ. Res. Inst. Math. Sci. (Kyoto)* **12** (2), 539–563.
Y. NAKANO (1978), *Water Resour. Res.* **14** (1), 125–134.
S. P. NEUMAN AND P. A. WITHERSPOON (1971), *Water Resour. Res.* **7** (3), 611–623.
J. T. ODEN, O. C. ZIENKIEWICZ, R. H. GALLAGHER, AND C. TAYLOR, Eds. (1974), "Finite Element Methods in Flow Problems," Univ. of Alabama Huntsville Press, Huntsville.
G. F. PINDER AND W. G. GRAY (1977), "Finite Element Simulation in Surface and Subsurface Hydrology," Academic Press, New York.
D. W. PRITCHARD (1971), *in* "Estuarine Modeling: An Assessment" (G. H. Ward, Jr., and W. H. Epsey, Jr., Eds.), Natl. Tech. Infor. Serv. Publ., #P8-206-807.
O. C. ZIENKIEWICZ (1971), "The Finite Element Method in Engineering Science," McGraw–Hill, New York.